

Article 6 :

Publié dans la revue *Engineering Research Express*.

- **Éditeur :** Institute of Physics Publishing
- **E-ISSN :** 2631-8695
- **Période de couverture par Scopus :** de 2019 à 2025
- **Domaine scientifique :** Génie général
- **Impact facture : 1.8 (2024);**
- **Lien d'article** [DOI 10.1088/2631-8695/ae1082](https://doi.org/10.1088/2631-8695/ae1082)
- **Type de source :** Revue scientifique (*Journal class B lien :* https://www.dgrstd.dz/fr/revues_B_st?revue=SCOPUS&search=Engineering+Research+Express)



A screenshot of the 'Moteur de recherche – Revues scientifiques' (Search Engine – Scientific Journals) interface. The top navigation bar includes 'Revues scientifiques', 'Liste des revues scientifiques de catégorie B', and 'Grands Domaines de Recherche en Sciences et Technologie'. A 'Scopus' button is visible. Below the search bar, there's a 'Scopus :1' indicator, a download icon labeled 'Télécharger', and a dropdown menu set to '20'. The search results table has columns for 'TITRE DE LA REVUE', 'EDITEUR', 'ISSN', and 'EISSN'. One result row shows 'Engineering Research Express' as the title, 'IOP Publishing Ltd.' as the editor, and '26318695' as the EISSN.



PAPER

Effect of transverse bottom slope and bed roughness on hydraulic jump flow in an asymmetrical trapezoidal stilling basin: an experimental approach

Seyfeddine Benabid*, Sonia Cherhabil, Abdelkader Ouakouak, Sid ali Djafri, Bedjaoui Ali and Taqiyeddine Assas

Published 15 October 2025 • © 2025 IOP Publishing Ltd. All rights, including for text and data mining, AI training, and similar technologies, are reserved.

[Engineering Research Express, Volume 7, Number 4](#)

Citation Seyfeddine Benabid *et al* 2025 *Eng. Res. Express* 7 045106

DOI 10.1088/2631-8695/ae1082

Article metrics

79 Total downloads

Submit

[Submit to this Journal](#)

Permissions

[Get permission to re-use this article](#)

Share this article



Article PDF

PAPER

Effect of transverse bottom slope and bed roughness on hydraulic jump flow in an asymmetrical trapezoidal stilling basin: an experimental approach

To cite this article: Seyfeddine Benabid *et al* 2025 *Eng. Res. Express* **7** 045106

You may also like

- [Modal interaction and energy harvesting response of a Bi-directionally excited piezoelectric vibration energy harvester](#)
M Saha, C Nikhil, P Nayak et al.
- [Triply periodic minimal surfaces for gradient impedance matching layers in ultrasonic transducers](#)
D D'Aprile, F Auricchio and S Morganti
- [Roughened bed stilling basin and its hydraulic jump characteristics](#)
Yakun Liu, Di Zhang, Jian Wu et al.

View the [article online](#) for updates and enhancements.

Engineering Research Express



PAPER

RECEIVED
19 May 2025

REVISED
27 September 2025

ACCEPTED FOR PUBLICATION
7 October 2025

PUBLISHED
15 October 2025

Effect of transverse bottom slope and bed roughness on hydraulic jump flow in an asymmetrical trapezoidal stilling basin: an experimental approach

Seyfeddine Benabid^{1,*}, Sonia Cherhabil¹, Abdelkader Ouakouak^{1,3}, Sid ali Djafri², Bedjaoui Ali¹ and Taqiyeddine Assas⁴

¹ Research Laboratory in Subterranean and Surface Hydraulic, LARHYSS, University of Biskra 7000, Algeria

² Research Laboratory of Civil Engineering, Hydraulics, Environment and Sustainable Development, LARGHYDE, University of Biskra, Biskra, Algeria

³ Faculty of Technology, University of El Oued, El Oued, PO, Algeria

⁴ Laboratory of Hydraulic Development and Environment, University of Biskra, Biskra, Algeria

* Author to whom any correspondence should be addressed.

E-mail: seyfeddine.benabid@univ-biskra.dz

Keywords: energy dissipation, non-rectangular stilling basin, hydraulic jump, dissipative elements

Abstract

Controlling hydraulic jump is critical for maximizing energy dissipation, minimizing erosion, and improving the performance of stilling basins. This study presents the first comprehensive experimental investigation of the combined effects of transverse bed slope and surface roughness on hydraulic jump characteristics, energy dissipation, and free-surface flow dynamics in an asymmetrical trapezoidal channel. An innovative stilling basin configuration was implemented, featuring a transversely inclined rough bed ($\theta = 17^\circ$) with vertical sidewalls and three distinct roughness heights (14.32, 24.47, and 30.76 mm), tested across a wide range of Froude numbers ($3.3 < F_1 < 9.4$). The experimental setup allowed the exploration of previously unexplored three-dimensional flow structures, revealing pronounced secondary turbulence that contributed significantly to energy dissipation. The results demonstrated that increasing bed slope and roughness substantially altered hydraulic jump behavior, reducing the sequent depth ratio by approximately 31.16% and the secondary depth by nearly 18.6% compared to classical jump. Additionally, the roller length decreased by an average of 39.11%, while greater slope and roughness height increased relative energy dissipation by 9.53% compared to a classical jump. Beyond the experimental work, new empirical relationships were developed to predict key hydraulic jump parameters, achieving error margins of $\pm 10\%$ to $\pm 20\%$ and closely matching the observed data, offering practical guidance for the design of efficient and resilient stilling basins.

List of symbols

| | |
|--------|--|
| g | Acceleration due to gravity [m/s^2]. V_1 Average velocity in section 1 [m/s]. |
| k_s | Relative roughness height [—]. k_e Roughness element height [mm]. |
| E_1 | Charge in the first section of the jump [m]. b Channel width [m]. |
| E_2 | Charge in the last section of the jump [m]. Q Flow discharge [m^3/s]. |
| d_1 | Average depth of upstream sequences [m]. A_2 Second section of water [m^2]. |
| d_2 | Average depth of downstream sequences [m]. A_1 First section of the water [m^2]. |
| D | Difference in transverse bed elevation [m]. f_1, f_2, f_3, f_4, f_5 Functional symbol. |
| ρ | Water density [kg/m^3]. μ Dynamic viscosity [$N.s/m^2$] |
| E_L | Energy loss associated with hydraulic jump [m]. x_l The jump toe position [m]. |

| | |
|--------------------|--|
| L_r shallow side | Length of the roller on the shallow side [m]. |
| L_r deeper side | Length of the roller on the deeper side [m]. |
| Y_1 | The initial depth of water flow in the horizontal channel [m]. |
| Y_2 | The second depth of water flow in the horizontal channel [m]. |

1. Introduction

In recent years, energy dissipation downstream of hydraulic structures has become a critical concern for engineers, as undissipated flow energy can scour the riverbed, potentially compromising dam stability and causing severe structural damage [1, 2]. At the heart of this challenge lies the hydraulic jump, a fundamental phenomenon for dissipating surplus kinetic energy. It is characterized by an abrupt transition from high-velocity supercritical flow to low-velocity subcritical flow, generating significant turbulence, surface waves and spray. This process underpins the design of flow energy dissipators and is commonly observed in structures such as weirs, stilling basins, and natural channels [3, 4].

The hydraulic jump has been the subject of extensive research since its first observation by Leonardo da Vinci. However, it remained poorly understood until the pioneering experimental work of Bélanger in 1820, who formulated the well-known Bélanger equation, which is still widely used to calculate the conjugate depth ratio in hydraulic jumps [5]:

$$\frac{d_2}{d_1} = \frac{1}{2}(\sqrt{1 + 8F_{r1}^2} - 1) \quad (1)$$

Where d_1 is the flow depth upstream, d_2 is the sequent flow depth and F_{r1} is inflow Froude number $F_{r1} = V_1 \sqrt{gd_1}$ in which V_1 is the supercritical flow velocity and g is the acceleration due to gravity.

Due to the high cost of constructing stilling basins, researchers have investigated methods to minimize sequent depth and jump length while enhancing turbulence to maximize energy dissipation. Modifying channel geometry and increasing bed roughness have proven effective in improving dissipation efficiency [6, 7]. One early study [8] examined hydraulic jump in a rectangular channel with a corrugated bed and introduced a roughness parameter $k_s = k_e/d_1$, where k_e represents the equivalent roughness. The results showed that, on a roughened bed, the downstream depth d_2 required for jump formation was considerably smaller than the corresponding sequent depth predicted by Bélanger's equation. Moreover, the hydraulic jump was markedly shorter than its conventional counterpart. More recently, [9] experimentally investigated hydraulic jump over both pebbled rough and smooth beds in a horizontal rectangular channel across a range of Froude numbers. Their results demonstrated that bed roughness decreased the sequent depth ratio, shortened the roller and aerated flow regions, and enhanced energy dissipation. Rough beds also exhibited stronger backflow and distinct air-entrainment patterns compared to smooth beds. In another contribution, [10] carried out experimental and theoretical studies on hydraulic jump to assess the combined effects of channel slope and bed roughness. Experiments were conducted on four slopes 0° to 6° and four roughness heights (10–30 mm). Results showed that increasing bed roughness enhanced energy dissipation by 29% and bed shear stress by 88%, while reducing the sequent depth ratio and relative jump length compared to smooth-bed and classical jumps. Similarly, [11] investigated hydraulic jump in sloped roughened channels, analyzing the influence of bed material size, slope, and relative roughness on jump height and dissipation efficiency. Their results indicated that higher slopes and roughness improved dissipation while shortening jump length, and practical design correlations were proposed based on the inflow Froude number. Subsequent studies extended this research to other channel geometries. For example, [12] conducted experimental investigations of hydraulic jumps in vertical U-shaped channels and developed predictive equations for downstream depth and limiting discharge. Their results revealed friction-induced deviations from classical hydraulic theory, offering valuable insights into the mechanisms of energy dissipation in curved and confined channels, which can inform more accurate design and optimization of hydraulic structures. [13] examined jumps in gradually expanding sloping channels with slopes of 0° – 6° and expansion ratios from 0.35 to 0.75. They found that increasing slope raised the sequent depth ratio and energy loss by up to 46% and 20%, respectively, while shortening jump length by up to 14%. Reducing the expansion ratio further improved energy dissipation. [14] investigated hydraulic jump in sloped compound rectangular channels with roughened minor beds. Tests with four positive slopes and five roughness levels, using uniform plastic pellets, showed that higher bed roughness reduced the sequent depth ratio and improved energy dissipation compared to smooth beds. Empirical equations linking the Froude number, depth ratio, relative roughness, and slope were proposed to support basin design in dams and irrigation systems. Furthermore, [15] examined jumps in abrupt asymmetric expanding stilling basins with various wall geometries and bed roughness levels. Their findings showed that roughness reduced the sequent depth,

jump length, and roller length relative to smooth prismatic channels, while enhancing stability and dissipation efficiency. [16] studied hydraulic jumps over roughened beds with negative slopes, employing gravel roughness heights of 1.25 cm and 2.2 cm under inflow Froude numbers ranging from 4.9 to 9.5. Results revealed that greater roughness increased energy dissipation by 11%, while reducing relative sequent depth by 16.6% and dimensionless jump length by 20.7%.

In open-channel hydraulics, trapezoidal channels play a vital role in water conveyance systems such as irrigation, drainage, and stormwater management. Both symmetrical and asymmetrical designs have been extensively studied. For instance, [17] was among the first to investigate hydraulic jump in symmetrical trapezoidal channels with 45° side slopes, demonstrating that the development of a bottom roller markedly affects flow dynamics and significantly improves energy dissipation efficiency compared to conventional rectangular channels. Similarly, [18] measured velocities in hydraulic jumps within a trapezoidal compound channel with 45° side slopes and developed machine learning models to predict these velocities, providing a robust and efficient method for estimating flow characteristics from limited experimental data. In contrast, [19] pioneered the study of hydraulic jump in asymmetrical trapezoidal channels with vertical sidewalls and a smooth, transversely sloping bottom, focusing on jump formation in such unique geometries. By varying channel width while maintaining a constant bottom slope, they identified three characteristic zones across the channel width: the shallow side, the center, and the deep side. Results showed a positive correlation between channel width and roller length on the shallow side, but an inverse correlation on the deep side, explained by the decreasing bottom slope as the channel narrows. Extending this line of inquiry, [20] conducted detailed velocity measurements in free-surface flow within a smooth asymmetrical channel to analyze unsteady three-dimensional dynamics, revealing complex flow structures that facilitate momentum exchange between the two sides of the channel. [21] conducted an experimental investigation of hydraulic jump in a smooth asymmetrical trapezoidal channel, focusing on the influence of sluice gate geometry specifically parallelogram and triangular types. Their results indicated that hydraulic jump in asymmetrical trapezoidal channel exhibited superior performance compared to those in triangular or symmetrical trapezoidal channels, particularly at higher Froude numbers, with parallelogram gates providing more efficient jump formation. [22] conducted theoretical and experimental investigations of hydraulic jumps in straight channels with non-uniform water depth by upstream sluice gates with non-rectangular profiles (toothed gates). By adapting and validating the Bélanger equation to these conditions, they achieved accurate predictions of jump height and energy dissipation under complex flow situations. The findings highlighted the strong influence of channel asymmetry and gate geometry on flow distribution, turbulence generation.

Although extensive studies on hydraulic jumps in channels with various geometries, no comprehensive assessment has yet been presented regarding the combined effects of transverse bed slope and bed roughness on jump behavior and energy dissipation. Previous research has primarily focused on symmetrical channels or channels with longitudinal slope and smooth, non-rectangular cross-sections, leaving a significant knowledge gap in understanding how transverse slope interacts with roughness to alter free-surface dynamics and generate a new flow mechanism. This mechanism involves the development of secondary flows and the intensification of turbulence generation, phenomena not observed in conventional designs, and represents a novel aspect in the study of hydraulic jump, particularly in relation to energy dissipation and jump stability. To address this gap, the present study experimentally investigates hydraulic jump in an asymmetrical trapezoidal channel with a transversely inclined and roughened bed. The results reveal a remarkable improvement in energy dissipation efficiency compared to conventional designs, achieved through a systematic evaluation of three different roughness configurations on a transverse slope of $\theta=17^\circ$. Furthermore, new empirical relationships for jump characteristics are developed, providing a comprehensive understanding of hydraulic jump dynamics and free-surface flow behavior in complex channel geometries. These findings contribute to the optimization of stilling basin design, enhancing performance and reducing erosion risks.

2. Materials and methods

The experimental study was carried out at the LARHYSS Laboratory, University of Biskra, using a rectangular flume constructed of metal and glass. The flume was 7.00 m long, 0.293 m wide, and 0.60 m high. Transparent glass panels were installed on the side walls to enable clear visual observation of flow behavior during the tests, as illustrated in figure 1.

The asymmetric trapezoidal cross-section of the channel was constructed by inclining the channel bed with Plexiglas panels at a transverse angle of $\theta = 17^\circ$ relative to the horizontal, as shown in figure 2. This slope was deliberately chosen as an intermediate value based on hydraulic principles, previous research findings, and practical experimental considerations, including channel setup, measurement instrumentation, and the precise control of flow variables. Prior studies [20, 21] were also consulted to ensure that the hydraulic jump formed

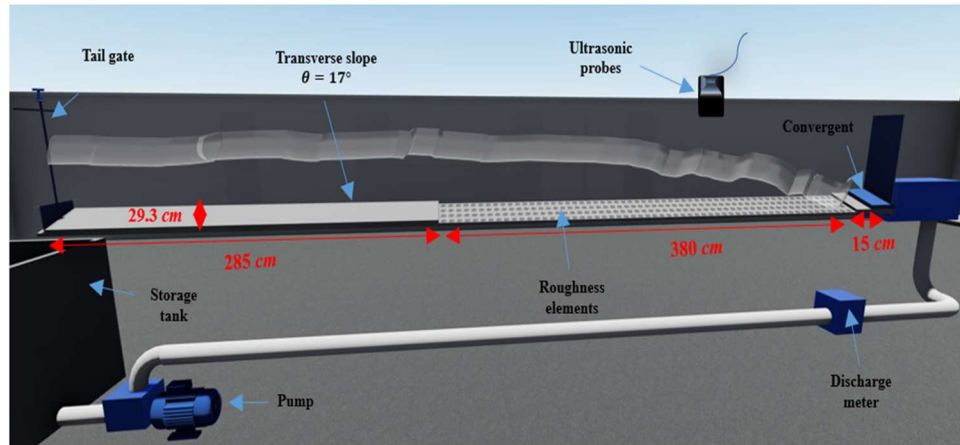


Figure 1. Schematic diagram of the experimental model setup.



Figure 2. Cross-section of the asymmetrical trapezoidal channel showing the transverse slope of the flume bottom.

with all its characteristic features, allowing an effective investigation of transverse flow effects. This intermediate slope provided favorable conditions for examining the influence of transverse slope on hydraulic jump behavior: smaller slopes would not generate sufficient lateral flow to adequately capture transverse mechanisms, whereas larger slopes could induce strong disturbances and increase the risk of local scour or erosion due to high flow intensity. To verify the effect of the transverse slope, a preliminary comparison was performed against the classical zero-slope configuration, which serves as a reference in most previous studies and enables a clear assessment of the selected slope's impact on hydraulic jump characteristics.

The experimental setup consisted of a hydraulic circuit designed for continuous flow recirculation. A circular pipe with a diameter of 125 mm connected the supply tank to the flume through a sealed metal box



Figure 3. Schematic illustrating the arrangement and configuration of roughness elements on the channel bed.

equipped with a precisely engineered convergent inlet, ensuring a uniform and sufficiently high initial flow depth d_1 . This configuration generated a steady, high-velocity supercritical flow, enabling the achievement of elevated Froude numbers. Experiments were conducted for three initial flow depths $d_1 = 0.03$, 0.035 and 0.04 m. In the downstream section, a movable vertical control valve was used to regulate the hydraulic jump toe position. Both smooth and rough bed conditions were tested to evaluate the influence of bed roughness on hydraulic jump characteristics and the associated energy dissipation efficiency.

To reproduce a rough channel bed, plastic panels were lined with crushed gravel and natural river pebbles and placed along the flume bottom beginning about 15 cm downstream of the inlet. The roughness elements were arranged and sized uniformly to maintain consistent conditions and ensure repeatability throughout all tests. Three roughness configurations were considered, each defined by an equivalent roughness height k_e as illustrated in figure 3. These roughness heights 14.32, 24.47 and 30.76 mm were selected to represent typical conditions encountered in energy dissipation basins, ranging from moderately rough concrete surfaces to highly rough natural beds. These values correspond to roughness scales commonly found in natural riverbeds and engineered dissipation structures, covering practical conditions from moderately rough concrete channels to highly roughened beds such as natural cobbles, in agreement with previous studies [10, 11, 23, 24]. The gravel was selected from various grain size classes (3/8, 8/15, 15/25, and 25/40 mm) and classified using standard sieve analysis. A granulometric study determined the median particle diameter d_{50} , defined as the size at which 50% of the sample is finer. The equivalent roughness height k_e was calculated by averaging the three orthogonal dimensions of individual gravel particles, following the methodology recommended in [23]. To ensure realistic interaction with the flow and minimize cavitation risks, the roughness layer was embedded flush with the adjacent upstream and downstream flume bed surfaces, preventing direct jet impingement on protruding elements, as shown in figure 3 [24]. The adoption of this methodology, consistent with that employed in previous studies, ensures methodological coherence and facilitates direct scientific comparison of the obtained results. However, despite the extensive literature on roughness effects, no prior research has specifically investigated how such roughness configurations influence the secondary flow mechanisms that generate turbulence and modify roller characteristics in hydraulic jumps.

During each modified experimental run, once steady flow conditions were established, the discharge Q was measured using an electromagnetic (EM) flowmeter (Krohne IFC 10D) with an accuracy of $\pm 0.5\%$ and a calibration precision exceeding 99.97%. The initial depth d_1 and sequent depth d_2 were recorded at three transverse positions across the channel (shallow side, centerline, and deep side) using three ultrasonic (US) probes (Microsonic). This configuration enabled precise measurement of water depths at the upstream and downstream boundaries of the hydraulic jump, with an accuracy of ± 1 mm. Due to pronounced free-surface fluctuations during testing, data were collected over 150 s at a sampling frequency of 1 Hz, and mean values were calculated for measurements along the two sidewalls and the centerline. To minimize the effect of free-surface fluctuations, temporal and spatial averaging was applied (i.e., averaging over time at each point and then across multiple transverse locations), effectively smoothing local oscillations and capturing a representative mean flow field. This approach reduced random variability and ensured that the reported data accurately represent hydraulic jump behavior. To capture variations in free-surface flow dynamics, additional surface elevation measurements were conducted along the channel at 10 cm intervals at the same three transverse positions. Sensors were mounted above the outer walls and moved smoothly along rails, allowing depth measurements at multiple locations along both the channel length and width, as illustrated in figure 4. The roller length L_r was measured separately on the deep and shallow sides using a graduated ruler fixed along the channel (± 1 mm resolution), defined as the horizontal distance from the point where the water surface rises abruptly

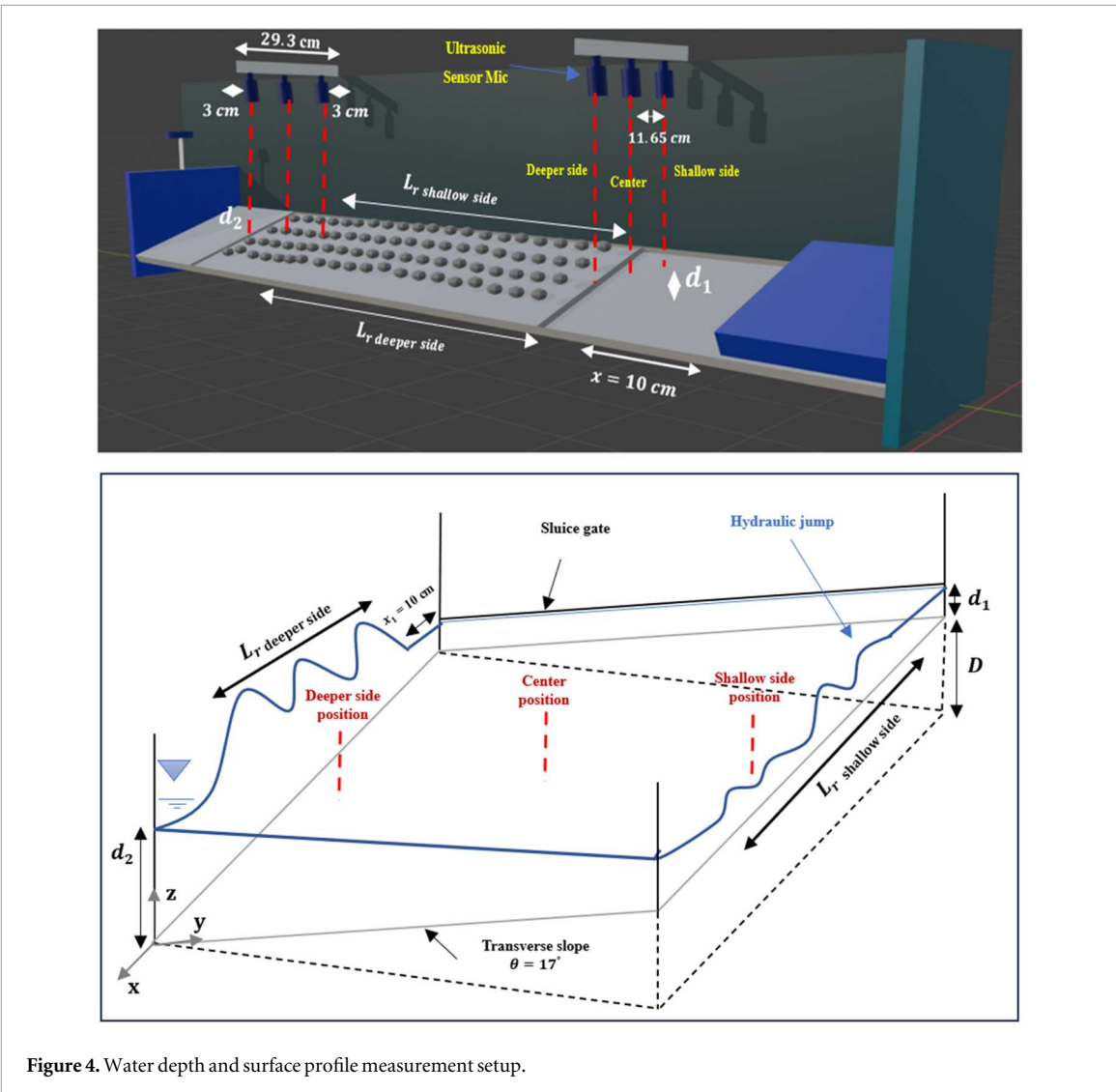


Figure 4. Water depth and surface profile measurement setup.

to where it stabilizes downstream. A dye tracer was introduced to facilitate clearer identification of the roller region.

Despite the use of high-precision instruments, measurement uncertainties of $\pm 0.5\%$ for discharge, $\pm 1\text{ mm}$ for depth, and $\pm 1\text{ mm}$ for roller length cannot be entirely eliminated. Preliminary error propagation analysis estimated a combined uncertainty of 2%–3% in the depth ratio and roller length. Additionally, model assumptions, such as steady flow and the neglect of minor lateral effects, may introduce systematic uncertainty, as in all previous studies, and were carefully considered during data interpretation to ensure that the reported results reliably represent hydraulic jump behavior. A summary of all measurements is presented in table 1.

A series of extensive experiments were conducted under varying flow conditions and downstream water depths. The discharge values ranged from 0.0242 to 0.0448 m^3/s , while the inlet Froude number ($F_{r1} = V_1 / \sqrt{gd_1}$) varied between 3.3 and 9.4. This range was deliberately selected to cover the Froude numbers reported in previous studies, thereby enhancing the general applicability of the results and providing a comprehensive understanding of hydraulic jump behavior under diverse conditions. The experimental data were analyzed using the principles of Froude and geometric similarity to ensure their relevance to practical flow scenarios and hydraulic structure design.

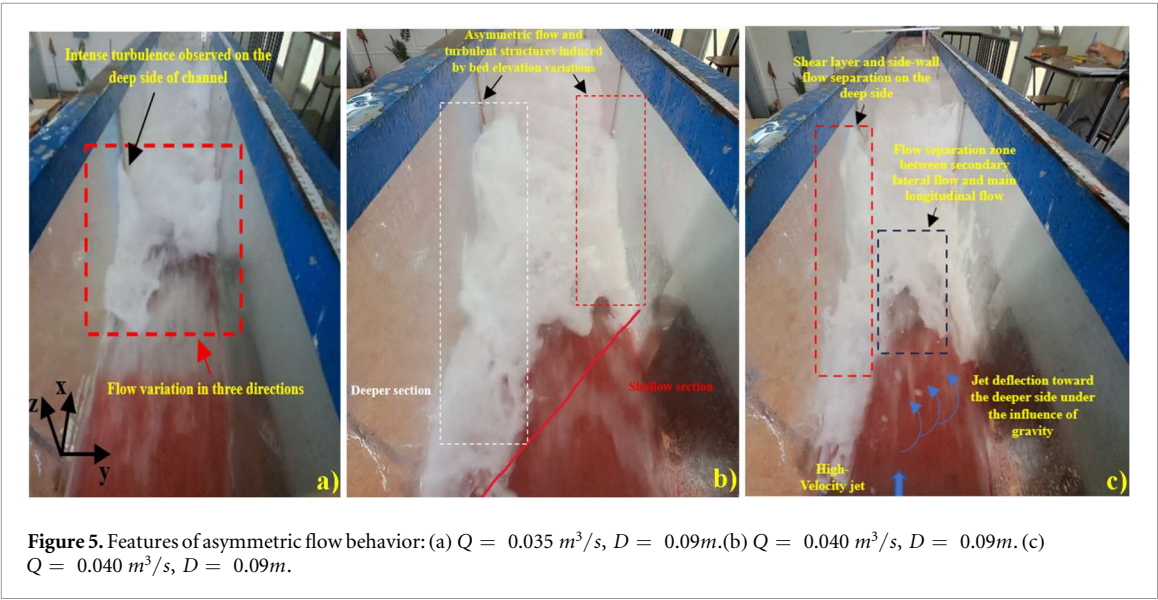
3. Dimensional analysis

In the case of an asymmetric trapezoidal channel, the factors governing the hydraulic jump phenomenon can be expressed through the following dimensional relationships:

$$f_l(d_1, d_2, g, \mu, \rho, V_1, k_e, D, L_r, E_L, E_1, E_2) \quad (2)$$

Table 1. Hydraulic jump test conditions.

| Channel | S. No | $d_1(m)$ | Roughnessheight ($k_e\text{mm}$) | Transverse slope (θ°) | F_r | $d_2(m)$ | $L_r/d_1\text{deoperside}$ | $L_r/d_1\text{shallowside}$ | $Q (m^3/s)$ |
|----------------------------------|-------|----------|------------------------------------|-------------------------------------|-----------|-----------|----------------------------|-----------------------------|-------------|
| Rectangular channel | A_1 | 0.03 | 0 | 0° | 6.01–9.15 | 0.25–0.38 | 32.68–51.42 | — | 0.031–0.043 |
| | A_2 | 0.035 | 0 | 0° | 4.24–7.58 | 0.18–0.35 | 19.26–42.15 | — | 0.024–0.041 |
| | A_3 | 0.04 | 0 | 0° | 3.25–6.67 | 0.17–0.37 | 14.17–38.07 | — | 0.025–0.033 |
| Asymmetrical trapezoidal channel | B_1 | 0.03 | 0 | 17° | 6.87–9.35 | 0.24–0.33 | 29.66–41.33 | 32.16–42.44 | 0.032–0.044 |
| | B_2 | 0.035 | 0 | 17° | 4.04–5.43 | 0.17–0.23 | 15.85–22.71 | 17.28–23.85 | 0.024–0.032 |
| | B_3 | 0.04 | 0 | 17° | 3.35–6.01 | 0.17–0.32 | 10.12–27.75 | 12.10–28.60 | 0.024–0.044 |
| Asymmetrical trapezoidal channel | C_1 | 0.03 | 14.32 | 17° | 5.11–8.54 | 0.14–0.25 | 17.33–33.16 | 18.66–34.66 | 0.024–0.042 |
| | C_2 | 0.035 | 14.32 | 17° | 4.10–7.44 | 0.13–0.27 | 13.28–30.28 | 12.42–30.71 | 0.024–0.044 |
| | C_3 | 0.04 | 14.32 | 17° | 3.31–4.47 | 0.12–0.19 | 8.12–15.50 | 9.75–14.75 | 0.024–0.032 |
| Asymmetrical trapezoidal channel | D_1 | 0.03 | 24.47 | 17° | 5.16–9.34 | 0.27–0.14 | 18.25–34.50 | 20.4–35.20 | 0.024–0.044 |
| | D_2 | 0.035 | 24.47 | 17° | 4.10–4.76 | 0.13–0.17 | 10.28–16.28 | 11.57–16.60 | 0.024–0.028 |
| | D_3 | 0.04 | 24.47 | 17° | 3.31–5.51 | 0.12–0.22 | 7.00–18.25 | 9.75–19.25 | 0.024–0.040 |
| Asymmetrical trapezoidal channel | E_1 | 0.03 | 30.76 | 17° | 5.18–9.40 | 0.13–0.24 | 16.5–32.54 | 17.30–33.83 | 0.025–0.044 |
| | E_2 | 0.035 | 30.76 | 17° | 4.10–7.41 | 0.13–0.23 | 11.42–25.40 | 12.4–27.42 | 0.024–0.044 |
| | E_3 | 0.04 | 30.76 | 17° | 3.30–6.07 | 0.10–0.23 | 7.50–19.05 | 8.00–20.37 | 0.024–0.044 |



Here, d_1 (m) average initial depth, d_2 (m) average final depth, g (m / s^2) gravity acceleration, μ (N.s/m^2) water viscosity, ρ (kg/m^3) water density, V_1 (m / s) average velocity, k_e (m) height of roughness, D the difference in transverse bed height ($D = 0.09\text{m}$), E_1 , E_2 (m) specific energy at the upstream and downstream of the hydraulic jump, L_r (m) the roller length. Using Buckingham's π -theorem of dimensional analysis and selecting d_1 , V_1 and ρ as the three repeated variables, a dimensionless functional relation can be derived, which is expressed as follows [11]:

$$f_2 = \left(\frac{d_2}{d_1}, R_{el} = \frac{V_1 d_1}{\mu}, F_{r1} = \frac{V_1}{\sqrt{g d_1}}, \frac{L_r}{d_1}, \frac{E_L}{E_1}, \frac{k_e}{d_1} \right) \quad (3)$$

Where, R_{el} represents the Reynolds number and F_{r1} the Froude number. Although the Reynolds numbers in this study ranged from 82.531 to 152.800, indicating that viscous effects can be neglected, the experiments were carried out at relatively large flow depths and channel dimensions. Under these conditions, the influence of surface tension on flow behavior and roller formation in the hydraulic jump is expected to be minimal compared to the dominant effects of inertia, turbulence, bed roughness, and transverse slope. Consequently, the values of the sequent depth ratio, relative roller length, and relative energy loss were determined as follows:

$$\frac{d_2}{d_1} = f_3 \left(F_{r1}, \frac{k_e}{d_1} \right) \quad (4)$$

$$\frac{L_r}{d_1} = f_4 \left(F_{r1}, \frac{k_e}{d_1} \right) \quad (5)$$

$$\frac{E_L}{d_1} = f_5 \left(F_{r1}, \frac{k_e}{d_1} \right) \quad (6)$$

Description of flow behavior

Experimental observations indicate that the hydraulic jump in this type of open channel exhibits characteristics that differ significantly from those in conventional symmetrical channels. Analysis of the free surface provides valuable insights into the three-dimensional flow dynamics and the complex behavior of the jump, as shown in figure 5(a). The transverse bed slope, under the effect of gravity, induces an asymmetric geometry that drives secondary flow from the shallow side toward the deep side, generating cross-channel circulation and pronounced differences in elevation, pressure, and turbulence. This drives water from the less dense regions toward the deeper side, increasing shear along the side walls. A flow separation zone forms between the lateral secondary motion and the main longitudinal flow, further modifying the velocity distribution across the channel, as illustrated in figure 5(b), (c). In addition, the deflection of the jet toward the deep side enhances interaction between different water layers and increases the thickness of the shear layer, thereby intensifying turbulence in this region of the hydraulic jump. This complex interaction between longitudinal and secondary flows contributes to effective energy dissipation, as the high kinetic energy is progressively converted into turbulence, vortices, and shear losses along the jump.

One of the key mechanisms contributing to this behavior is the clear difference in the surface roller dynamics between the two sides. On the deeper side, the roller is shorter and more turbulent due to redirected

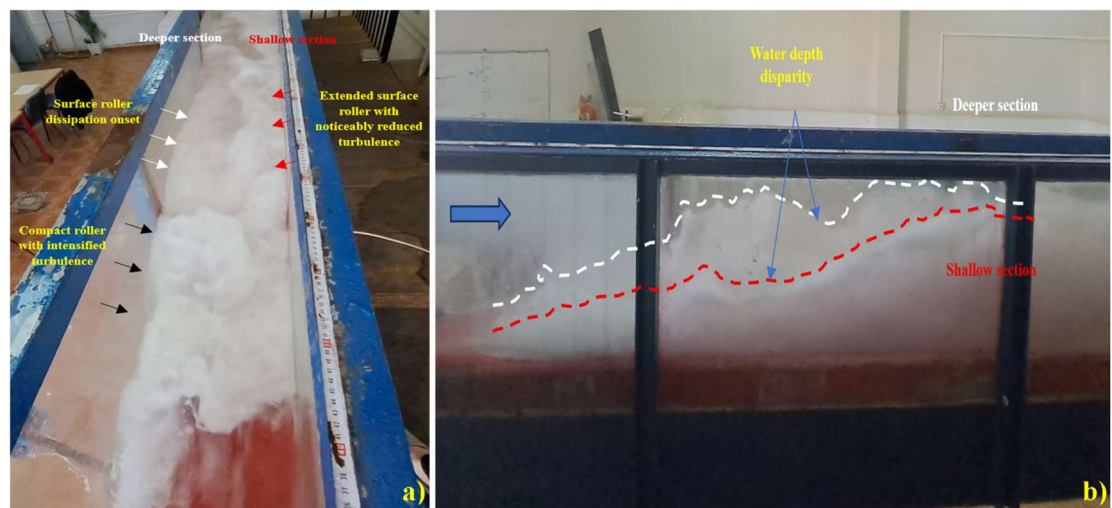


Figure 6. Roller structure and turbulence variation in an asymmetric hydraulic jump: $Q = 0.040 \text{ m}^3/\text{s}$, $D = 0.09\text{m}$.

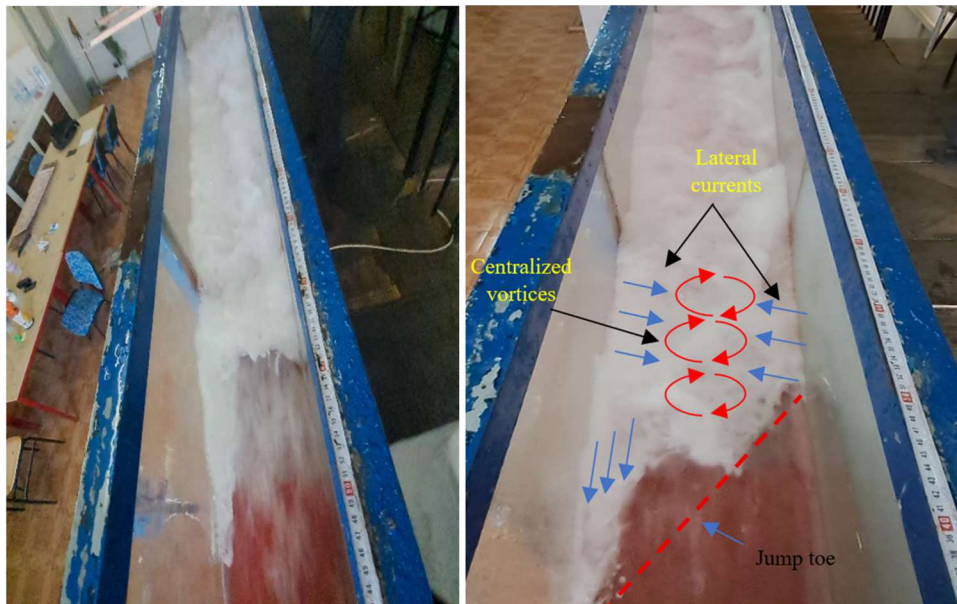


Figure 7. View showing the asymmetric arrangement of the hydraulic jump toe under high discharge conditions: $Q = 0.034\text{m}^3/\text{s}$, $D = 0.09\text{m}$.

momentum and elevated turbulence levels, which accelerate energy dissipation and reduce the kinetic energy available for its development, as shown in figure 6(a). This side is also characterized by a greater water depth compared to the shallow side, as illustrated in figure 6(b). On the shallow side, however, the roller retains relatively more energy and extends farther, but exhibits a lower turbulence level due to the reduced depth and weaker shear forces compared to the deeper side. This behavior is attributed to the influence of secondary lateral currents, which redistribute momentum and enhance flow energy dissipation, highlighting the critical role of the transverse bed slope in shaping hydraulic jump dynamics.

The most important observation in this channel is that, under high-flow conditions, the hydraulic jump forms in the deepest section, where a clear asymmetry appears at the jump toe, as shown in figure 7. This asymmetry results from the complex interaction between the high-velocity flow and secondary lateral currents along the channel walls, leading to the formation of a strong central vortex that shifts the jump toe toward the deepest section. These hydraulic interactions increase resistance, reduce local velocities, and significantly redistribute the flow within the channel, enhancing the understanding of hydraulic jump behavior in asymmetric sections.

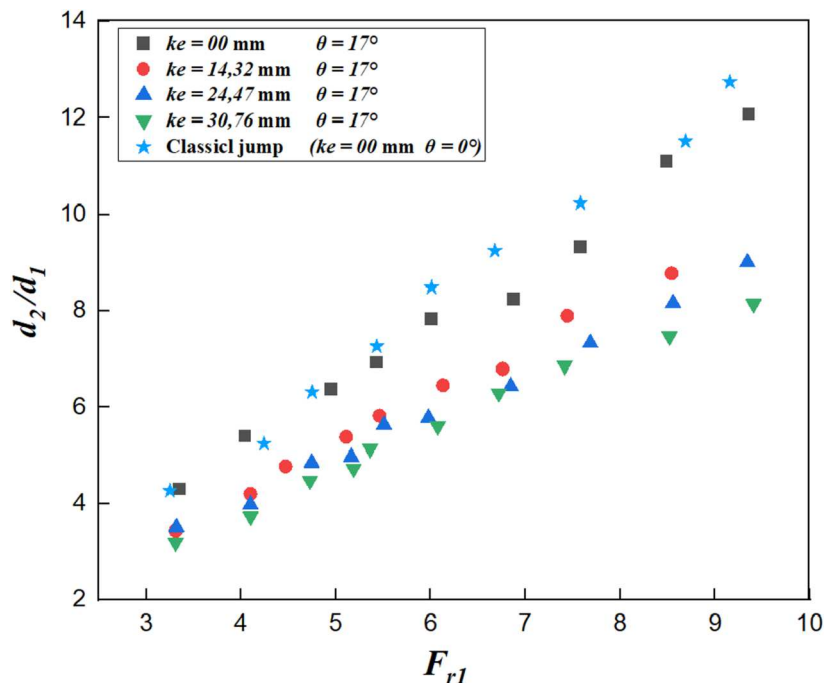


Figure 8. Variation of the sequent depth ratio (d_2/d_1) as a function of the inflow Froude number (F_{r1}) for various bottom roughness heights (k_e).

4. Results and discussion

This section analyzes the key hydraulic jump parameters sequent depth ratio, roller length, relative energy dissipation, and free-surface flow profiles selected in line with prior research and standard hydraulic engineering practices to ensure a comprehensive and practically relevant assessment. The functional forms describing these parameters were derived from the theoretical principles governing hydraulic jump behavior and supported by previous experimental studies, ensuring methodological consistency, comparability, and alignment with established scientific approaches.

4.1. Depth ratio

To investigate the effect of dissipation factors on the sequent depth ratio of the hydraulic jump (d_2/d_1). Figure 8 illustrates the variation of depth ratio values (d_2/d_1) with the Froude number (F_{r1}) for different bottom roughness heights (k_e).

As observed in all experiments, an increase in the incoming Froude number (F_{r1}) results in a corresponding linear increase in the sequent depth ratio (d_2/d_1). However, the introduction of bed roughness elements combined with the transverse bottom slope led to a significant reduction in this ratio compared to hydraulic jumps on sloping smooth beds and to classical jumps under the same Froude number conditions. To precisely evaluate the effects of both roughness and transverse slope, the analysis was carried out separately for each roughness and slope configuration at the same Froude number, and the results were then compared with those obtained on smooth beds and in classical jumps. Based on these comparisons, the average reduction in the sequent depth ratio was calculated, amounting to 28.34% relative to sloping smooth beds and 31.16% relative to classical jumps. This highlights the combined influence of bed roughness and transverse slope. Moreover, it was found that increasing the roughness height and slope intensity resulted in an additional decrease in the sequent depth ratio, reflecting their decisive role in enhancing secondary currents, intensifying turbulence, and promoting flow separation. This analysis was carried out with high precision for each Froude number within every roughness configuration, with averages calculated to represent the characteristic response, thereby enhancing the reliability of the results and strengthening the credibility of the conclusions. Visual observations during the experiments revealed that increasing the height of the roughness elements promoted the formation of vortices and localized flow recirculation between these elements. Additionally, the transverse bed slope induced a lateral displacement of the flow from the shallow side toward the deep side, which intensified the secondary currents. These complex flow structures are likely responsible for the increased turbulence and flow separation, ultimately leading to the significant reduction in the sequent depth ratio.

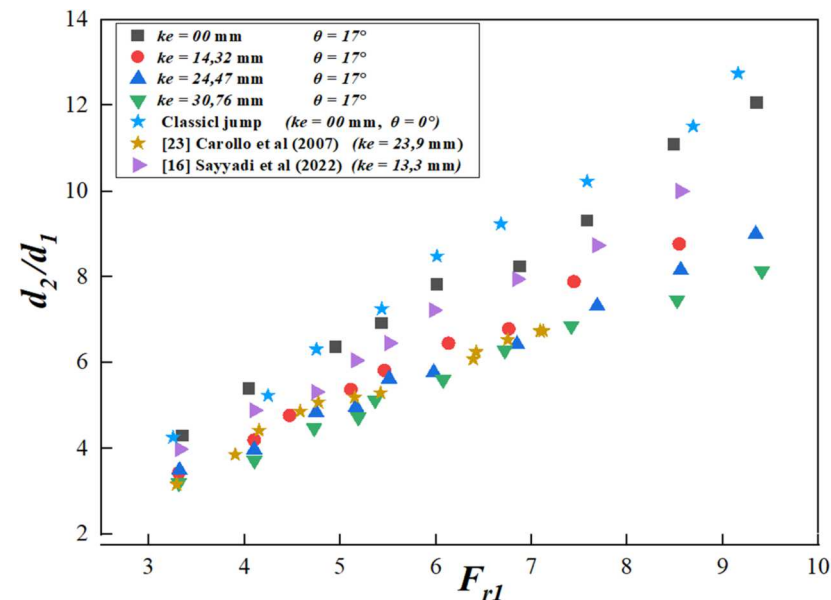


Figure 9. Comparison of values (d_2/d_1) obtained in the present study with results reported in previous research.

The present study compared the sequent depth ratio with data from previous experimental investigations [16, 23], as shown in figure 9. The results exhibit strong agreement with those of [23], where a roughness height of $k_e = 23.9 \text{ mm}$ was used, closely matching the present study's value of $k_e = 24.47 \text{ mm}$ for comparable Froude numbers. In contrast, when compared with the findings of [16], which employed a roughness height of [16], which employed a roughness height of $k_e = 13.3 \text{ mm}$, the present study with $k_e = 14.32 \text{ mm}$ reported sequent depth ratios (d_2/d_1) approximately 24% lower. This difference highlights the significant influence of both bed roughness characteristics and the transverse slope of the channel bottom on hydraulic jump behavior.

Based on the experimental findings, the following empirical equation is proposed to predict the sequent depth ratio (d_2/d_1) as a function of the initial Froude number (F_{r1}) and the relative roughness height (k_e/d_1):

$$\frac{d_2}{d_1} = \left(-0, 3948 \frac{k_e}{d_1} + 1, 2414 \right) F_{r1} + 0.271 \quad (7)$$

Figure 10 presents a comparison between the sequent depth ratios predicted by the empirical equation (7) and those obtained from laboratory measurements. The results also show close agreement with previous studies [10, 25], confirming the reliability of the experimental approach. The proposed equation reproduces the observed data with an error margin not exceeding $\pm 10\%$, reflecting its robustness and practical applicability for estimating the sequent depth ratio. Although some sources of uncertainty such as measurement limitations and model assumptions are inherent to experimental research, their influence in this study was systematically minimized to maintain the accuracy of the results within acceptable limits, thereby ensuring that they do not compromise the reliability of the findings or the validity of the conclusions drawn.

[24] introduced a dimensionless parameter D to quantify the reduction in sequent depth, defined as $D = (d_2^* - d_2)/d_2^*$, where d_2^* represents the sequent depth of a hydraulic jump over a smooth bed under identical upstream flow conditions. The relationship between D and the initial Froude number, based on the experimental results, is presented in figure 11. The results show that the maximum reduction in sequent depth, approximately 38.17%, occurred at a roughness height of 30.76 mm.

4.2. Relative roller length

Another important characteristic of the hydraulic jump is the surface roller length (L_r/d_1). Figure 12 illustrates the variation of the relative roller length with the inflow Froude number (F_{r1}) on both the shallow and deep sides of the channel, taking into account different bed roughness heights (k_e).

The study identifies two distinct roller zones in the asymmetrical trapezoidal channel, generated by the transverse flow between the shallow and deep sides (secondary flow). This finding supports the observations reported by [19, 21, 22], who identified the formation of two roller types on both sides of the channel in smooth-bed conditions. The roller behavior observed in this study highlights the unique three-dimensional flow structures induced by the channel's asymmetry and transverse slope features absent in symmetrical or rectangular channels.

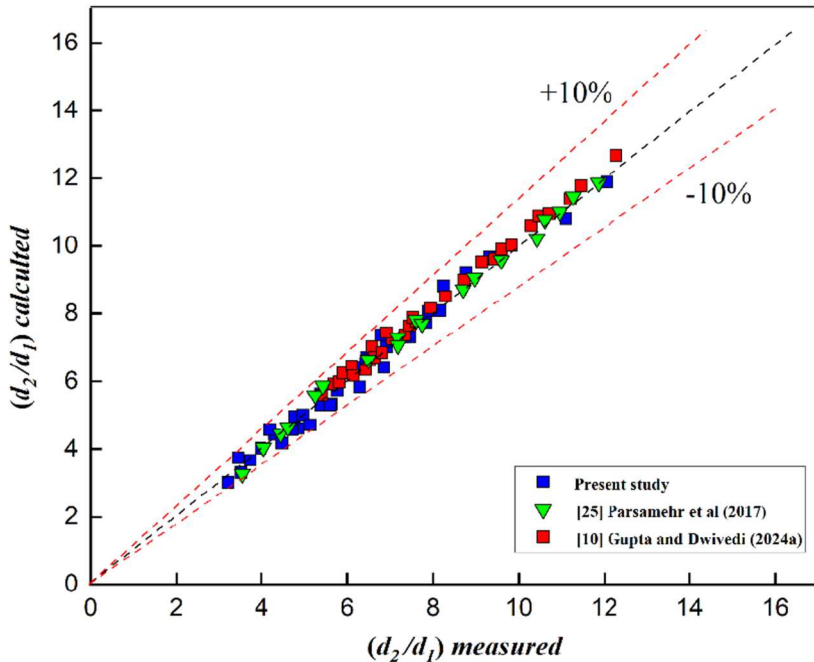


Figure 10. Comparison between measured values and those calculated using equation (7) for the depth ratio (d_2/d_1).

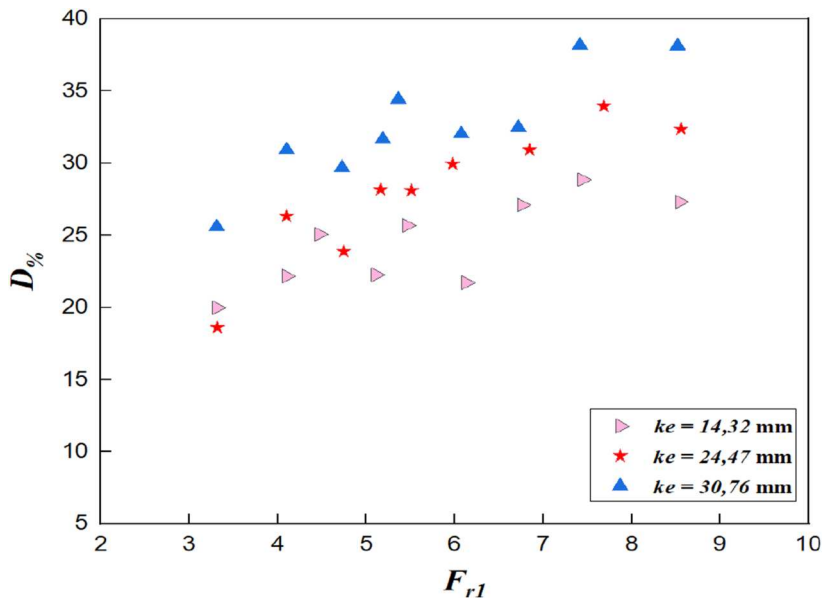


Figure 11. Variation of the dimensionless depth deficit parameter (d_2/d_1) as a function of the inflow Froude number (F_{r1}).

Figure 12 shows that the relative roller length (L_r/d_1) increases with the inflow Froude number (F_{r1}) on both the shallow and deep sides, indicating a stronger hydraulic jump at higher flow intensities. However, it decreases with increasing bed slope and roughness height, with the most significant reductions of 42.8% and 40%, respectively recorded for the rough-bed configuration with a roughness height of $k_e = 30.76\text{mm}$ and a slope of $\theta = 17^\circ$. In addition, the roller length on the deeper side is about 7.5% shorter than on the shallower side, emphasizing the asymmetric effect of channel geometry on jump behavior.

The combination of the transverse bed slope and increased roughness disrupts the main flow, generating secondary currents and localized turbulence between the shallow and deep sides. These secondary flows redirect part of the flow's momentum from the shallow side toward the deep side, creating two distinct rollers. The roller on the deeper side is shorter because the redirected momentum and enhanced turbulence accelerate energy dissipation, leaving less kinetic energy available to sustain its development. In contrast, the shallow-side roller retains more energy, allowing it to extend further. Compared to smooth or flat-bottomed channels, these

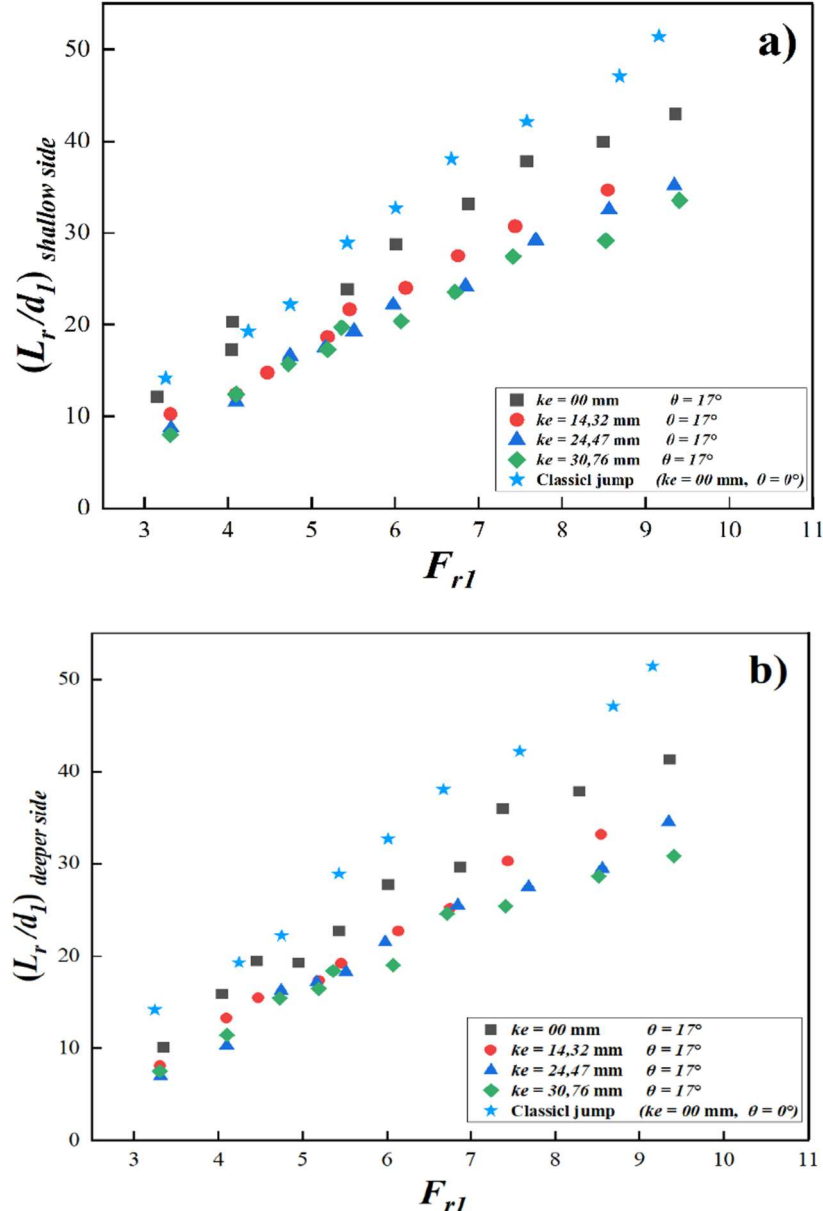


Figure 12. Variation of the relative roller length (L_r/d_l) against Froude number (F_{r1}) under various roughness heights (k_e): (a) Shallow side, (b) Deeper side.

mechanisms enhance turbulent energy dissipation, promote faster roller formation and stabilization, and reduce the overall roller length. The intensified turbulence and improved mixing redistribute momentum more effectively, converting a larger portion of the flow's kinetic energy into heat and vortical motion. This explains both the observed difference in roller sizes and the increased energy loss within the jump region.

Based on the analysis of the experimental data, empirical relationships were established to estimate the relative roller length on both the shallow and deep sides of the channel.

$$L_r/d_{l\text{shallow side}} = \left(-1.055 \frac{k_e}{d_l} + 5.218 \right) F_{r1} - 4.769 \quad (8)$$

$$L_r/d_{l\text{deeper side}} = \left(-1.183 \frac{k_e}{d_l} + 5.224 \right) F_{r1} - 5.315 \quad (9)$$

Figure 13 illustrates the comparison of relative roller lengths on the shallow and deep sides of the channel, as determined from the empirical equations (8) and (9) and validated against experimental observations. The outcomes are in strong agreement with earlier investigations [23, 26], confirming the consistency of the findings. The proposed empirical relationships replicate the measured data with deviations not exceeding $\pm 20\%$, underscoring their reliability and suitability for describing hydraulic jumps in asymmetric channel

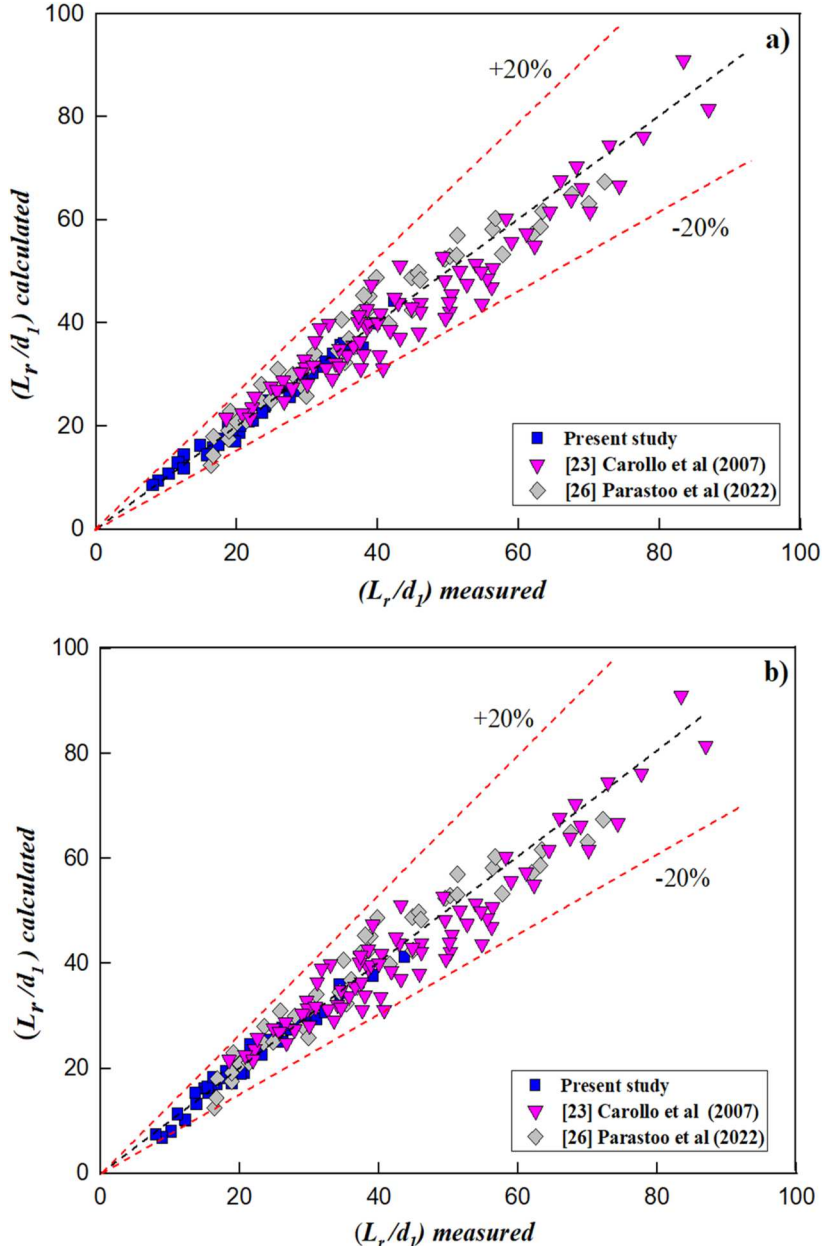


Figure 13. Difference between measured and calculated values in the relative roller length (L_r/d_1): a) Shallow side equation (8), b) Deeper side equation (9).

configurations. While uncertainties arising from measurement processes and modeling assumptions are inevitable in experimental studies, their impact in the present work was carefully controlled and kept within acceptable bounds. As a result, the credibility of the results and the soundness of the conclusions remain unaffected.

According to [23], empirical formulations were developed to estimate the relative roller length (L_r/d_1) as a function of the sequent depth ratio in hydraulic jumps. The derived expressions establish the relationship between these parameters as follows:

$$\frac{L_r}{d_1} = 4.078 \left(\frac{d_2}{d_1} - 1 \right) \quad (10)$$

$$\frac{L_r}{d_1} = \frac{2.048}{\left(\frac{d_1}{d_2} \right)^{1.272}} \quad (11)$$

In this study, roller length was measured experimentally to verify the applicability of equations (10) and (11) for predicting roller length in an asymmetrical trapezoidal channel. Figures 14 and 15 present the experimental data pairs (L_r/d_1 , $(d_2/d_1) - 1$) and (L_r/d_1 , d_1/d_2) for different roughness heights on the shallow and

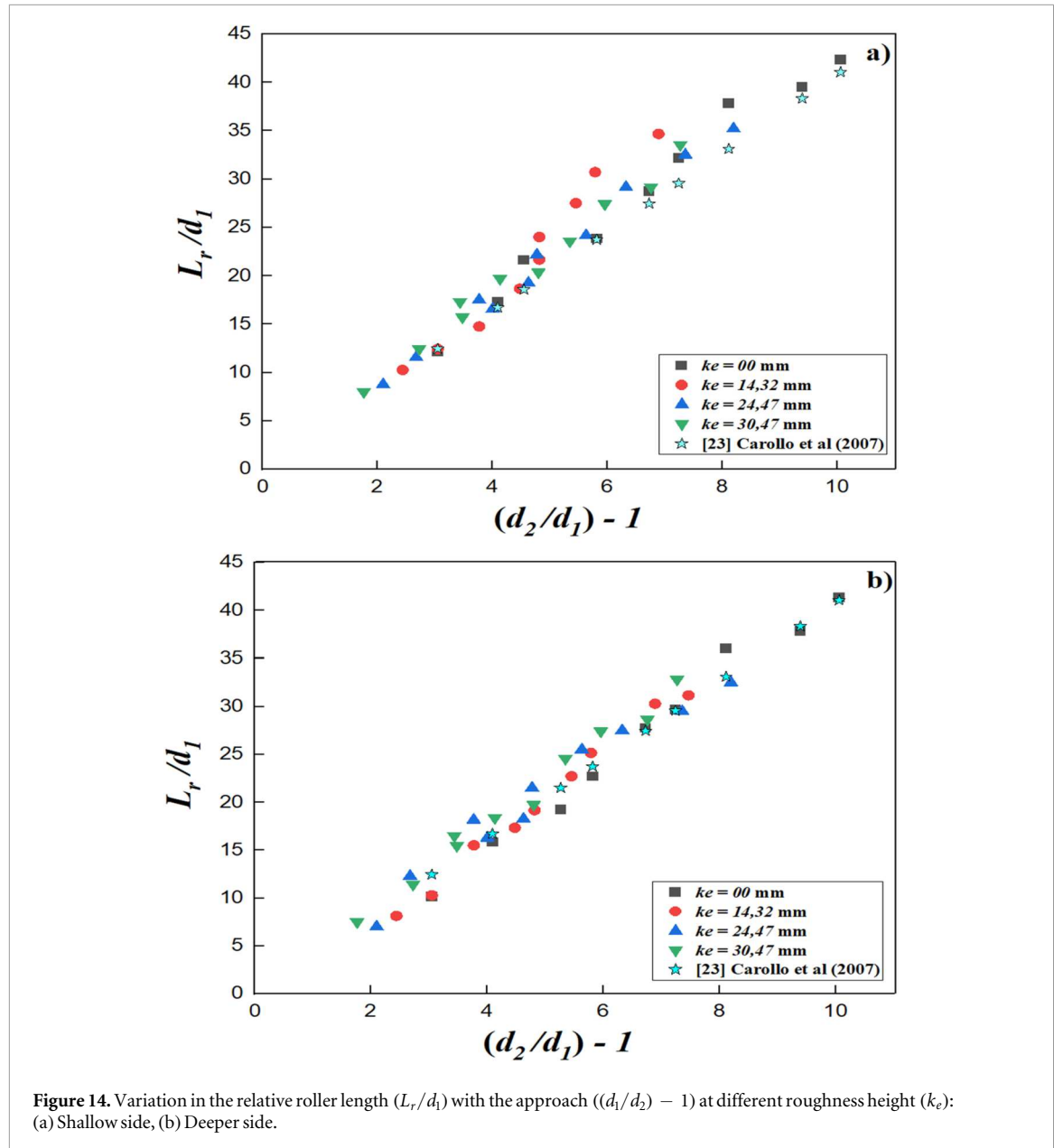


Figure 14. Variation in the relative roller length (L_r/d_1) with the approach ($(d_1/d_2) - 1$) at different roughness height (k_e):
(a) Shallow side, (b) Deeper side.

deep sides of the channel. Figure 14 shows that (L_r/d_1) increases almost linearly with $((d_2/d_1) - 1)$, indicating that roller length grows proportionally with the relative increase in sequent depth. In contrast, figure 15 indicates that (L_r/d_1) decreases rapidly as (d_1/d_2) increases, showing that a larger depth ratio corresponds to a shorter roller length, likely due to the contraction of the energy dissipation zone. These distinct trends emphasize the complex relationship between flow depth ratios and roller length during a hydraulic jump. The close agreement of the experimental data with the empirical relationships proposed by [23] further validates the predictive capability of these models. The consistent results across varying roughness conditions confirm the robustness of the data for characterizing roller length in asymmetrical trapezoidal channels with rough beds.

Based on the current data, a relationship-based model equation for the pairs of $(L_r/d_1, (d_2/d_1) - 1)$ and $(L_r/d_1, d_1/d_2)$ was formulated as indicated below equations (12–15).

$$\frac{L_r}{d_1}_{\text{shallow side}} = 4.768 \left(\frac{d_2}{d_1} - 1 \right) - 1.348 \quad (12)$$

$$\frac{L_r}{d_1}_{\text{shallow side}} = 2.325 \left(\frac{d_1}{d_2} \right)^{-1.2447} \quad (13)$$

$$\frac{L_r}{d_1}_{\text{deeper side}} = 4.447 \left(\frac{d_2}{d_1} - 1 \right) - 1.496 \quad (14)$$

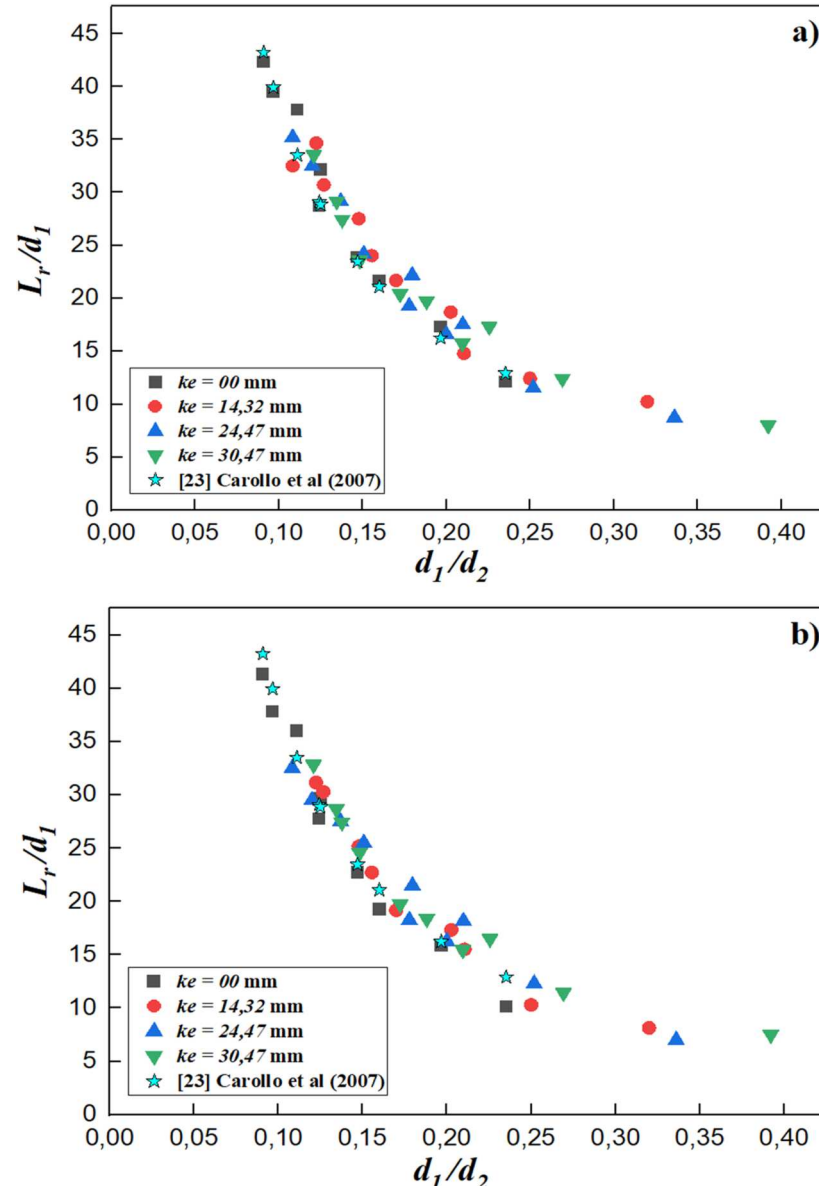


Figure 15. Variation in the relative roller length (L_r/d_1) with the approach (d_1/d_2) at different roughness height (k_e): (a) Shallow side, (b) Deeper side.

$$\frac{L_r}{d_1}_{\text{deeper side}} = 1.816 \left(\frac{d_1}{d_2} \right)^{-1.3582} \quad (15)$$

4.3. Relative energy loss

Energy dissipation through intense turbulence is the fundamental mechanism governing a hydraulic jump. The general expression for the relative energy loss (E_L/E_1) in a hydraulic jump is given by equations (16) [21]:

$$\frac{E_L}{E_1} = \frac{E_1 - E_2}{E_1} = \frac{d_1 + \frac{Q^2}{2gA_1^2} - d_2 + \frac{Q^2}{2gA_2^2}}{d_1 + \frac{Q^2}{2gA_1^2}} \quad (16)$$

In the asymmetric trapezoidal channel context, $A_1 = b \cdot d_1$ is the area of the initial wetted section for a rectangular gate of the convergent and, $A_2 = b \cdot (d_2 - D/2)$ is the area of the final section of the jump.

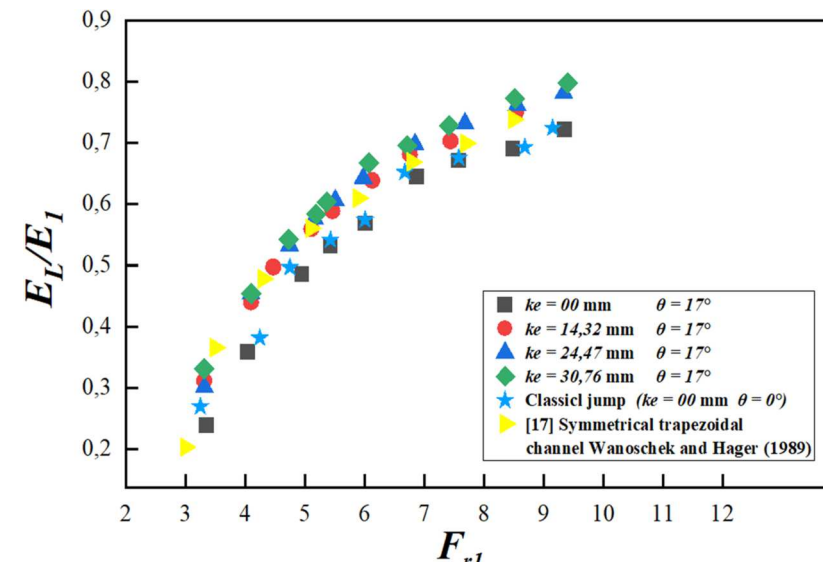


Figure 16. Variation of relative energy loss (E_L/E_I) versus Froude number (F_{rI}) for different roughness heights (k_e).

By using the general efficiency relationship. As depicted in equation (17):

$$\frac{E_L}{E_1} = \frac{1 - \frac{d_2}{d_1} + \frac{F_{rI}^2}{2} \left(1 - \frac{A_1^2}{A_2^2} \right)}{1 + \frac{F_{rI}^2}{2}} \quad (17)$$

Figure 16 presents the values of relative energy loss (E_L/E_I), calculated using equation (17), as a function of the inlet Froude number (F_{rI}) for various roughness heights (k_e) as well as for smooth bed. These results are compared with those of a classical hydraulic jump and a symmetrical trapezoidal channel [17].

Figure 16 shows that, for the same inflow Froude number (F_{rI}), the relative energy loss ratio (E_L/E_I) is significantly higher in the asymmetrical trapezoidal channel with a rough bed compared to the smooth bed condition ($k_e = 00 \text{ mm}$). This enhancement in energy dissipation becomes more pronounced with increasing bed roughness, reaching a maximum increase of 8.5% for the rough bed configuration ($k_e = 30.76 \text{ mm}$, $\theta = 17^\circ$).

The roughness elements disturb the boundary layer and amplify shear at the bed interface, promoting the development of turbulent structures. They induce localized velocity gradients that generate vortices, intensifying turbulence and enhancing mixing throughout the flow. Moreover, the transverse bed inclination generates secondary currents perpendicular to the main flow, redistributing momentum and facilitating wave breaking. The combined effects of bed roughness and inclination increase flow resistance, create recirculation zones, and accelerate the onset of fully developed turbulence in the hydraulic jump region. Consequently, the intensified turbulence, enhanced mixing, and greater flow resistance collectively explain the observed increase in energy dissipation, emphasizing the critical role of inclined rough beds in controlling hydraulic jump dynamics.

This study is compared with the classical hydraulic jump and the previous findings of [17]. The results indicate that, for inflow Froude numbers in the range $3.1 < F_{rI} < 5.1$, the hydraulic jump efficiency in both asymmetrical and symmetrical trapezoidal channels is comparable, yet notably higher than that observed in classical jumps. However, for higher inflow Froude numbers $5.1 < F_{rI} < 8.6$, the efficiency in asymmetrical channels with rough beds is significantly greater than in both classical and symmetrical configurations. These findings underscore the critical influence of channel geometry and bed roughness in enhancing hydraulic jump efficiency and energy dissipation.

4.4. Water surface profile

Figure 17 presents the average variations of the hydraulic jump surface profile, obtained by averaging the measurements from the shallow side, center, and deep side of the channel, for different relative roughness heights $k_e = 00, 14.32, 24.47$, and 30.76 mm .

Figure 17 highlights the influence of bed conditions on the behavior of the hydraulic jump. In all configurations tested, the jump produced a clear rise in water depth; however, a distinct pattern was observed when comparing rough and smooth beds. The introduction of surface roughness consistently reduced the

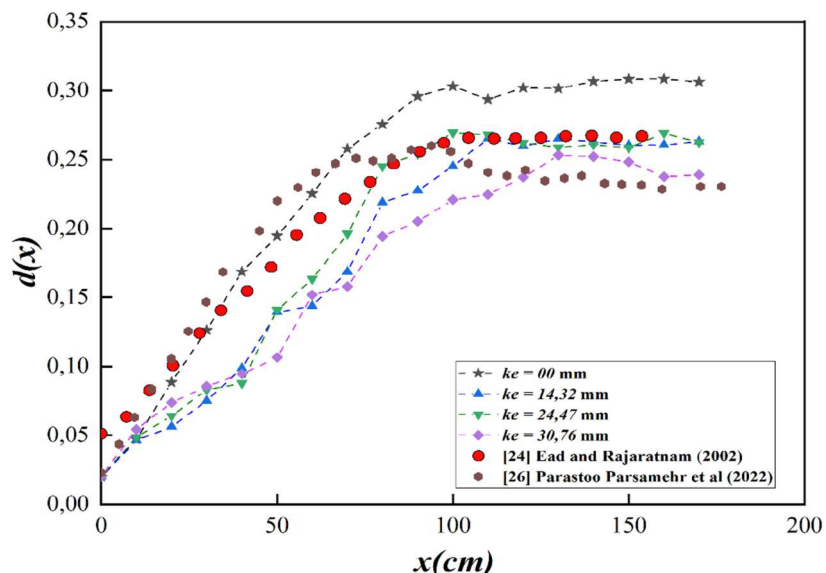


Figure 17. Variations in hydraulic jump surface profiles for different rough bed configurations.

downstream water depth, and this reduction became more pronounced as the height of the roughness increased. These findings are consistent with previously reported results [24, 26]. The magnitude of this reduction was quantified as approximately 9.2%, 17.8%, 18.8%, and 24.9% for the respective roughness configurations. Similarly, the effect of roughness was not limited to water depth. Increasing the roughness height also shortened the length of the hydraulic jump, with the smallest jump length recorded at the maximum tested roughness of 30.76 mm. This shortening can be explained by the enhanced flow resistance and energy dissipation generated by the roughness elements, which disrupt the flow structure and reduce the momentum transfer downstream. In addition, the water surface over rough beds displayed noticeable disturbances, particularly near the jump toe. This phenomenon is attributed to the interaction between the incoming flow and the roughness elements, which promotes the formation of vortices, intensifies turbulence, and creates localized zones of flow separation. These combined effects lead to improved energy dissipation and result in a more compact and hydraulically efficient jump.

5. Statistical evaluation and examination of equation sensitivity

Statistical evaluation and sensitivity analysis are essential for assessing the accuracy, reliability, and predictive capability of empirical models, as well as for quantifying uncertainty and validating derived relationships [11]. In this study, curve fitting was performed using widely adopted tools (OriginPro and Microsoft Excel), with the choice of linear or nonlinear regression determined by the nature of each relationship. Model parameters were estimated using the Least Squares Method, which minimizes the total sum of squared deviations between observed and predicted values, thereby enhancing the robustness and credibility of the developed correlations in representing hydraulic jump behavior. To achieve a comprehensive analysis, 50 data points were collected for each hydraulic jump characteristic including the sequent depth ratio, relative roller length, and energy dissipation efficiency. Nine experiments were conducted for each bed configuration to cover a wide range of conditions. For the surface profile measurements, 18 data points were recorded for each configuration at 10-cm intervals along the channel, providing sufficient spatial resolution to accurately capture hydraulic behavior. This distribution and number of experimental runs provided a solid foundation for reliable sensitivity analysis of the derived equations. Predicted results were systematically compared with experimental data, confirming the reliability and robustness of the correlations. The performance of the empirical equations describing the sequent depth ratio and relative roller length on both sides of the hydraulic jump in an asymmetric trapezoidal channel with a rough bed was evaluated using three key statistical indicators: the coefficient of determination (R^2), root mean square error (RMSE), and mean absolute error (MAE) were used to measure model accuracy. The results are summarized in table 2.

Table 2. Statistical evaluation and sensitivity analysis of empirical correlations for hydraulic jump characteristics.

| Equations | Target variable | Input parameters | R ² | RMSE | MAE | Sensitivity remarks |
|---------------|---|------------------|----------------|-------|-------|--|
| Equation (7) | Depth ratio d_2/d_1 | $k_e/d_1, F_r$ | 0.982 | 0.273 | 0.227 | Highly accurate, roughness and inflow Froude number strongly influence depth ratio. |
| Equation (8) | Relative roller length L_r/d_1 (shallow side) | $k_e/d_1, F_r$ | 0.983 | 1.16 | 0.92 | Strong sensitivity to both bed roughness and flow intensity. |
| Equation (9) | Relative roller length L_r/d_1 (deeper side) | $k_e/d_1, F_r$ | 0.975 | 1.362 | 1.14 | Good fit, increased complexity slightly reduces accuracy. |
| Equation (12) | Relative roller length L_r/d_1 (shallow side) | d_2/d_1 | 0.958 | 1.83 | 1.43 | Acceptable model using only sequent depth ratio. |
| Equation (13) | Relative roller length L_r/d_1 (shallow side) | d_1/d_2 | 0.964 | 1.689 | 1.345 | Nonlinear form, better than equation (12) but slightly less robust than roughness-based. |
| Equation (14) | Relative roller length L_r/d_1 (deeper side) | d_2/d_1 | 0.991 | 1.06 | 0.873 | Highest accuracy overall, depth ratio is a reliable predictor. |
| Equation (15) | Relative roller length L_r/d_1 (deeper side) | d_1/d_2 | 0.943 | 2.08 | 1.47 | Acceptable, nonlinear nature leads to larger errors. |

$$R^2 = \left[\frac{n \sum X_{exp} X_{cal} - (\sum X_{exp})(\sum X_{cal})}{\sqrt{(\sum X_{exp}^2 - (\sum X_{exp})^2)(\sum X_{cal}^2 - (\sum X_{cal})^2)}} \right]^2 \quad (18)$$

$$RMSE = \sqrt{\frac{\sum_{i=1}^n (X_{exp} - X_{cal})^2}{n}} \quad (19)$$

$$MAE = \frac{1}{n} \sum_{i=1}^n |X_{exp} - X_{cal}| \quad (20)$$

In these equations, X_{exp} refers to the observed data point, X_{cal} indicates the corresponding predicted value, and n represents the total number of data points.

As shown in table 2, equation (7) demonstrates excellent predictive capability, with R^2 of 0.982, $RMSE$ of 0.273 and MAE of 0.227. This underscores the strong influence of both bed roughness and inflow conditions on the evolution of flow depth within the hydraulic jump region. Equations (8) and (9), which predict the relative roller length (L_r/d_1) on the shallow and deep sides, respectively, based on (k_e/d_1) and (F_{r1}) , also exhibit high performance ($R^2 = 0.983$ and 0.975). These results highlight the sensitivity of roller length to upstream flow energy and bed roughness, confirming their importance as key controlling parameters. Furthermore, equations (12) and (13) for the shallow side, and equations (14) and (15) for the deep side, express roller length in terms of the sequent depth ratio using both linear and power-law formulations. Among these, equation (14) achieved the highest overall accuracy ($R^2 = 0.9913$), indicating that the linear correlation with (d_2/d_1) is highly robust for modeling roller development. Equation (13) also showed good performance ($R^2 = 0.964$), while equation (15), which employs a power-law formulation, exhibited slightly lower accuracy ($R^2 = 0.943$), with higher $RMSE$ and MAE values (2.08 and 1.47, respectively), likely due to the increased complexity and non-linearity of the model.

It should be emphasized that these equations are valid only within the range of experimental conditions investigated, including the studied Froude number range and the asymmetric trapezoidal channel geometry, and should be applied with caution beyond these conditions.

6. Conclusion

This study systematically investigated the combined effects of a transversely inclined bottom and a rough bed on the main characteristics of hydraulic jumps in an asymmetrical trapezoidal stilling basin using large-scale experiments. Empirical formulas were developed to predict the sequent depth ratio and relative roller length, with error margins of $\pm 10\%$ and $\pm 20\%$, providing reliable tools for practical design applications. The results demonstrated that the hydraulic jump developed complex three-dimensional turbulent structures, generating pronounced secondary flows that significantly enhanced energy dissipation and influenced the main jump characteristics. The combined effects of bed roughness and transverse slope produced substantial reductions in the sequent depth ratio d_2/d_1 , averaging 28.34% compared to a smooth inclined bed and reaching 31.16% relative to the classical hydraulic jump. Similarly, the relative roller length L_r/d_1 on both shallow and deep sides was considerably shorter than in a smooth inclined bed, with maximum reductions of 27.67% and 20.31%, and reaching 40.73% and 37.49% relative to the classical jump. Relative energy loss E_L/E_1 increased significantly with transverse bed roughness, exceeding the levels recorded in the classical jump and symmetrical trapezoidal channels, particularly at higher Froude numbers, with average increases of 9.53% and 7.03%, highlighting the crucial influence of bed slope and roughness on energy dissipation. These findings provide practical guidance for designing highly efficient stilling basins capable of dissipating energy, reducing erosion, and enhancing the stability of hydraulic structures under diverse operational and climatic conditions. They also establish a foundation for developing sustainable water resource management strategies that support the creation of more efficient, resilient, and environmentally responsible hydraulic infrastructures, directly contributing to the achievement of sustainable development goals.

Limitation of the study

The experiments were conducted on a scaled-down model as part of the first comprehensive experimental investigation of an asymmetric trapezoidal channel with a transversely inclined and rough bed, focusing on the fundamental mechanisms of the hydraulic jump. Hydraulic similarity, rather than full geometric similarity, was adopted to ensure an accurate representation of the dominant forces (gravity and inertia) and to preserve the physical behavior of the jump within a Froude number range of 3.3 to 9.5. This approach provides reliable

insights into the hydraulic jump dynamics, although some scale-related effects may exist, such as differences in Reynolds number and turbulence intensity between the model and a full-scale prototype. The geometric, velocity, and Froude scale ratios were carefully chosen to minimize these effects, ensuring that the results remain reliable and applicable to real-world structures. To further enhance the engineering applicability of the findings, future research should include larger-scale experiments or field studies incorporating variations in bed slope, channel width, and bed roughness density. Additionally, CFD simulations can be employed to solve the Navier–Stokes equations using appropriate turbulence models, track the free surface, and validate numerical predictions against experimental or field data.

Author's contribution:

Benabid S: Conceptualization, analysis and interpretation of data, writing—review & editing. **Cherhabil S:** Conceptualization, writing—review & editing. **Ouakouak A:** writing - review & editing. **Djafri S A:** figure generation, revision and editing. **Bedjaoui A:** Creation, revision, and refinement of figures. **Assas T:** figure generation, revision and editing.

Acknowledgments

The authors would like to express their sincere appreciation to the LARHYSS laboratory -University of Biskra-, the Water Resources Foundation of BATNA, and the DGRSDT-Algeria- for their support in the realization of this work.

Conflict of interest

The authors declare that they have no conflict of interest.

Data availability statement

The datasets generated during and/or analysed during the current study are available from the corresponding author on reasonable request.

References

- [1] Hasanabadi H N, Kavianpour M R, Khosrojerdi A and Babazadeh H 2023 Experimental study of natural bed roughness effect on hydraulic condition and energy dissipation over chutes *iranian Journal of Science and Technology - Transactions of Civil Engineering* **47** 1709–21
- [2] Trinh C T and Tran C T 2025 Numerical and analysis effects of rectangular prism rough beds on hydraulic jumps in open channels *AIP Adv.* **15** 1–10
- [3] Müller G 2025 Theoretical model for the onset condition of a steady hydraulic jump *J. Hydraul. Res.* **63** 278–82
- [4] Simsek O, Akoz M S and Oksal N G S 2023 Experimental analysis of hydraulic jump at high froude numbers *Sadhana - Academy Proceedings in Engineering Sciences* **48** 47
- [5] De Padova D and Mossa M 2021 Hydraulic jump a brief history and research challenges *Water* **13** 1733
- [6] Pourabdollah R, Heidarpour M and Abedi Koupari J 2019 An experimental and analytical study of a hydraulic jump over a rough bed with an adverse slope and a positive step *iran J. Sci. Technol. - Trans. Civ. Eng.* **43** 551–61
- [7] Daneshfaraz R, Sammen S, Norouzi R, Abba S, Salem I, Mirzaee A, Sihag R and Elbeltagi P 2024 Estimating the effect of sand-roughened bed on hydraulic jump characteristics using heuristic models results *In Engineering* **23** 102724
- [8] Pourabdollah N, Heidarpour M and Abedi Koupari J 2019 An experimental and analytical study of a hydraulic jump over a rough bed with an adverse slope and a positive step *iranian Journal of Science and Technology - Transactions of Civil Engineering* **43** 551–61
- [9] Bahmanpouri F, Gaultieri C and Chanson H 2023 Flow patterns and free-surface dynamics in hydraulic jump on pebbled rough bed *Proc. Inst. Civ. Eng. Water Manage.* **176** 32–49
- [10] Gupta S K and Dwivedi V K 2024 A effect of surface roughness and channel slope on hydraulic jump characteristics: an experimental approach towards sustainable environment *iranian Journal of Science and Technology - Transactions of Civil Engineering* **48** 1695–713
- [11] Gupta S K and Dwivedi V K 2024b Experimental investigation of hydraulic jump characteristics in sloping rough surfaces for sustainable development *Eng. Res. Express* **6** 025103
- [12] Cherhabil S, Bedjaoui A and Benabid S 2025 Experimental study of the limiting flow discharge and the main characteristics of the hydraulic jump in a vertical 'U' shaped channel *Tuijin Jishu* **46** 951–63
- [13] Gupta S K and Dwivedi V K 2025 Experimental evaluation of hydraulic jump characteristics in gradually expanding sloping channel *J. Appl. Fluid Mech.* **18** 1843–60
- [14] Ibtissam H, Samir K, Ali G, Haroun K and Djamel B 2025 Experimental investigation of the sequent depth ratio in hydraulic jumps occurring in a sloped compound rectangular channel with a rough minor bed *Water Pract. Technol.* **20** 1745–62
- [15] Torkamanzad N, Dalir A H, Salmasi F and Abbaspour A 2019 Hydraulic jump below abrupt asymmetric expanding stilling basin on rough bed *Water* **11** 1–29

- [16] Sayyadi K, Heidarpour M and Ghadampour Z 2022 Effect of bed roughness and negative step on characteristics of hydraulic jump in rectangular stilling basin *Shock Vib* **2022** 1–12
- [17] Wanoscuk R and Hager W H 1989 Ressaut hydraulique en canal trapézoïdal *J. Hydraul. Res.* **27** 429–46
- [18] Bouriche F, Debabcche M, Carvalho R F and Djeddou M 2023 Velocity distribution in a controlled hydraulic jump in a compound channel: an experimental and machine learning (ML) study *Larhyss J.* **54** 217–37
- [19] Rodriguez-Diaz A J 1954 The hydraulic jump in a non-rectangular open channel *Master's Thesis* Georgia Institute of Technology. Directed by Mr Carstens
- [20] Kiri U, Leng X and Chanson H 2020 Positive surge propagating in an asymmetrical canal *J. Hydro-environ. Res.* **31** 41–7
- [21] Debabcche B and Cherhabil S 2024 Study of a hydraulic jump in an asymmetric trapezoidal channel with different sluice gates *Fluid Dynamics & Materials Processing* **20** 1499–516
- [22] Debabcche B 2025 Theoretical and experimental study of the transverse water depth hydraulic jump *PhD thesis, University of Biskra, Algeria*. Department of Civil Engineering and Hydraulics, University of Biskra, Algeria Supervised by Sonia Cherhabil
- [23] Carollo F G, Ferro V and Pampalone V 2007 Hydraulic jumps on rough beds *Journal of Hydraulic Engineering* **133** 989–99
- [24] Ead S A and Rajaratnam N 2002 Hydraulic jumps on corrugated beds *J. Hydraul. Eng.* **128** 656–63
- [25] Parsamehr P, Davoud F, Dalir A H, Abbaspour A and Esfahani M J 2017 Characteristics of hydraulic jump on *Rough Bed with Adverse Slope ISH Journal of Hydraulic Engineering* **23** 301–7
- [26] Parsamehr P, Kuriqi A, Farsadizadeh D, Dalir A H, Daneshfaraz R and Ferreira R M L 2022 Hydraulic jump over an adverse slope controlled by different roughness elements *Water Resour. Manage.* **36** 5729–49